Journal of
Mechanical
Science and
Technology

Journal of Mechanical Science and Technology 21 (2007) 1957~1963

Satic states of cohesive granular media

I. Preechawuttipong[1,*], R. Peyroux[2], F. Radjai[2] and W. Rangsri[1]

[1]*Department of Mechanical Engineering, Chiang Mai University, Chiang Mai 50200, Thailand*
[2]*Laboratoire de Mécanique et Génie Civil, CNRS-Université Montpellier II, Montpellier 34095, France*

(Manuscript Received August 14, 2006; Revised May 15, 2007; Accepted May 25, 2007)

Abstract

This paper investigates the influence of cohesion on the behavior of 2D granular media simulated by using a molecular dynamics method, involving a simple contact law with adhesion. The study considers an adhesion index which is non intrinsic but significant for interpreting the mechanical effects of applied pressure. A static state system of 4000 particles is numerically simulated by oedometrical compression under a constant force, without gravity. The results show how the geometrical texture and the network of contact forces change according to the level of adhesion. This effect is explained essentially in term of the increase in the number of the tensile contacts and by the development of the internal self-stress structure. As in the case of non cohesive granular media, a high spatial heterogeneity of the contact forces is observed.

Keywords: Granular material; Adhesion; Molecular dynamics; Texture.

1. Introduction

A granular material is defined as a collection of solid particles for which the macroscopic behavior is governed by contact interaction forces. We find many examples of granular media, notably in the civil engineering domain: soil, concrete and also in fragmentation processes. In the agro-product, pharmaceutical and chemical industry, many products are constituted from grains or powders. The macroscopic and microscopic properties of granular media are generally complex. Many experimental or numerical studies on the mechanical behavior of granular packing have been undertaken over the last thirty years, with the aim to predict the macroscopic behavior of a granular medium, and to investigate the grain scale or the contact scale. Such studies have indicated that if the whole medium is dense, then it tends to be strongly structured. This conclusion was first arrived at from contact force network analysis, and noting in particular its inhomogeneous nature [1], and secondly from the study of the contact directions which characterize the non isotropy of the contact network [2-4].These investigations were focused primarily on non cohesive granular media.

The aim of this work is to study, by numerical simulation, the evolution of the texture of granular systems under progressively increasing surface energy (adhesion) between grains, starting with a non cohesive medium. By "texture" we mean both force and contact networks for a multi-contact system. In cohesive granular packing, the cohesion arises form attraction forces with various physio-chemical origins that inhibit the loss of contacts, together with elastic contact deformation that allows a pair of particles in contact to support compressive forces (up to the point of cracking particle).

In this paper, we first present a simple model of adhesion between two circular particles. We define then an "adhesion index" that represents the activation of attractive forces compared to repulsive forces. After a short description of the numerical sample and of the boundary conditions, we present our main results

*Corresponding author. Tel.: +66 53 94 41 46, Fax.: +66 53 94 41 45
E-mail address: ittichai@dome.eng.cmu.ac.th

regarding forces, the coordination number, the statistics of contact directions and tensile pressure as functions of the adhesion index. We also study the evolution of specimen density.

2. Adhesion model

In molecular dynamics and most popular *discrete element* simulation methods, the particles are treated as rigid bodies [5, 6] moving according to Newton's equations of motion [7]. Classically, the contact force is defined as the function of the particles positions and velocities. In our numerical algorithm, we introduced a model of adhesion between two particles in contact characterized by an overlap δ and a contact surface $2a$; Fig.1. At first order in δ/r, the radius of the contact zone is given by $a = \sqrt{r\delta}$. This dependence is generally non-linear as in Hertzian contact analysis for example.

Consider firstly the normal effect of adhesion on contact. The adhesion is introduced as a resistance to a separation effort. With an idea similar to the model of adhesion on a solid surface of JKR [8, 9], we establish an interaction model between two particles in which the contact force is the sum of a repulsion effort and an adhesion effort. We select a simple linear elastic law for the repulsion component $k\delta$, where k is the contact stiffness, and an attraction force proportional to the contact surface $2a$ given by $\gamma\sqrt{r\delta}$, where γ represents the surface energy of particles in contact and r the effective radius of the curvature of the interface when $\delta = 0$. The dynamic effects are taken into account with a viscous damping term $\alpha_n\dot{\delta}$, where α_n is a normal damping coefficient. So, the expression for the normal force f_n as a function of δ is given by:

$$f_n = k\delta + \alpha_n\dot{\delta} - \gamma\sqrt{r\delta} \tag{1}$$

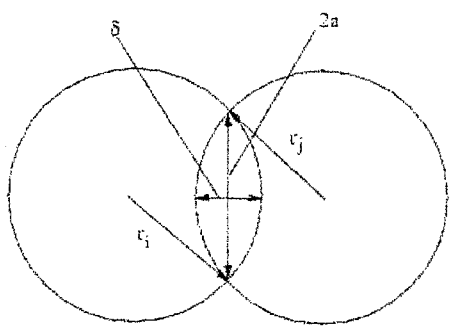

Fig. 1. Geometry of the contact between two disks.

In the following, this model will be called the "*Geometrical Adhesion model*" (GA).

The dependence of normal contact force the overlap δ is presented in Fig. 2. We can distinguish behavior on either side of the equilibrium position: $\delta_{eq} = r\gamma^2/k^2$, that occurs without applied external force and corresponds to no interactive effort: A compression zone exists for $\delta > \delta_{eq}$ and a tensile zone for $\delta < \delta_{eq}$. Note that the threshold tensile force (necessary force for separating two particles in contact) in this model is given by $F_c = r\gamma^2/4k$ with corresponding overlap $\delta_c = r\gamma^2/4k^2$. The zone between 0 and δ_c is an unstable zone which if reached would lead to separation following an imposed displacement or effort.

The implementation of Coulomb's law in the molecular dynamics approach poses a fundamental technical difficulty for numerical investigation, i.e. different coefficients of dynamic and static friction, [10, 11]. In fact, the integration of the equation of motion requires a "smooth" force law such that the friction force f_t is a function of the slide velocity v_t. According to Coulomb's law of friction, the set of permissible pairs between f_t and v_t cannot be represented as a (single-valued) "nonsmooth" function. A simple way to avoid this difficulty is to adopt a "regularized" form of the exact Coulomb's law with adhesion defined by (Fig. 3)

$$f_t = \min\left\{\beta|v_t|, \mu(f_n + F_c)\right\}\mathrm{sign}(v_t) \tag{2}$$

Here μ represents a coefficient of friction and β is a tangential viscosity. The latter should be given a value large enough to avoid numerical artifacts [10, 12]. Note that in the present model, the overlap is permitted.

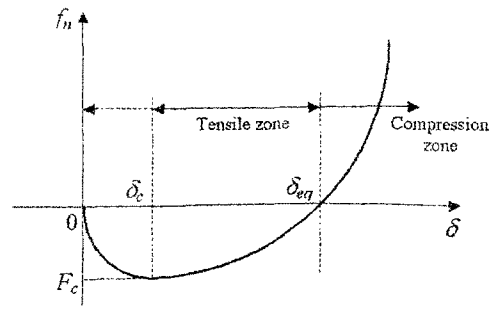

Fig. 2. Evolution of normal force f_n as a function of overlap depth δ for the AG model in the quasi-static case.

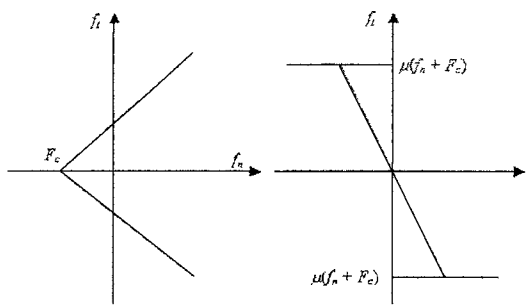

Fig. 3. Regularized Coulomb's law with adhesion.

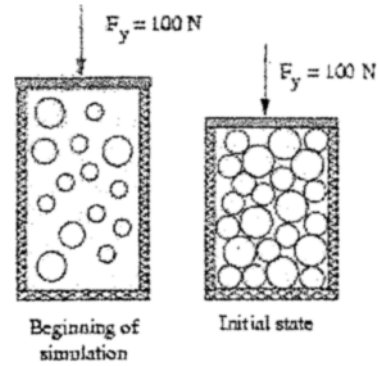

Fig. 4. Scheme of the preparation of the numerical samples.

A force law with adhesion in a broad sense involves a pair of adjacent particles resisting not only normal separation, but also relative sliding and rolling. When these conditions are fulfilled, the interparticle contact is *cemented*, i.e. the variables for the degrees of freedom of the particles in contact are frozen within a range of supportable forces and moments. However, we will not consider here the rolling friction and stiffness so that contiguous particles may freely roll on one another with no bending moments acting between them.

Since the influence of adhesion is expected to depend only on the *relative* amount of attraction with respect to repulsion, we define the dimensionless quantity η referred to as the "adhesion index" and being the ratio of the mean attraction force $\gamma\sqrt{r\delta}$ to the mean repulsion force $k\delta$ in a multicontact particle assembly. In the quasi-static case, for our model

$$\eta = \frac{\langle \gamma\sqrt{r\delta} \rangle}{\langle k\delta \rangle} \tag{3}$$

This adhesion index gives a measure of the effective cohesion of a granular medium at a given stage of its evolution. It's value can be small even with strong adhesion between particles if the compression loading is large compared with the adhesion threshold. We can note that η is an increasing function of F_c. According to the expression of the stress tensor in terms of contact forces, the average normal force $\langle f_n \rangle$ has the same sign as the average pressure p [13, 14]. Eq. (3) shows that if the average pressure is positive, i.e. for a system that is globally in compression, then $\eta \in [0,1]$, whereas for a system globally in traction we have $\eta \in [1,2]$. In the absence of external forces, where the repulsive force term = 0 for all contacts, and more generally if pressure is zero, we have $\eta = 1$.

3. Numerical sample

Numerical simulations were carried out on a 2D sample by using the molecular dynamics method based on the predictor-corrector scheme with Gear's set of corrector coefficients for the integration of the equations of motion [7].

The 2D samples were composed of 4000 disks with average radii equal to 3 mm. The radii are uniformly distributed between 2 and 4 mm. The particles were randomly distributed (triangular network) in a box of four rigid plane walls and gravitational effects were neglected. The stiffness and the coefficient of damping were the same for all particle-particle and particle-box contacts. A vertical force of 100 N was then applied on the upper wall. The others walls, during this stage, were fixed. The system was then allowed to relax until a static equilibrium was reached. The final state of this preparation stage is used as the initial equilibrium state for our analysis (Fig. 4). The adhesion and the friction between particles were activated from the beginning of each simulation. The adhesion between disks and rigid planes was taken as zero.

4. Numerical results

Various cases were considered in the simulation in term of the microscopic parameters. The various macroscopic variables investigated were found to depend on the degree of adhesion introduced through the adhesion surface energy γ. Here these results will be interpreted through their dependence on the adhesion index η. It is of-interest to examine the geometric texture of the media in terms of the coordination number, the compactness and the anisotropy that evolves from the preparation process. We study also the distribution of the normal contact forces in the

sample to quantify the influence of the adhesion at microscopic level.

Coordination number: The coordination number z is defined as the average number of contacts per particle. The coordination number z increases with η to stagnate around 4 for η = 0.3 (Fig. 5(a)). For η between 0.3 and 0.8, z increases very slightly, but is still close to 4, but the fraction of tensile contacts (z^-/z) increases (Fig. 5(b)). For the high values of η, z increases more rapidly. The highest value of z 4.3 is reached for the non-friction case.

Contact directions: In order to achieve a better analysis of the contact network, we present the statistical distribution $p(\theta)$ of the normal directions θ of contact which is the probability density to have a contact oriented in a given direction θ [15]. Here we present the polar diagram of the number of contacts $N_p(\theta)$ as a function of their direction θ, in 18 angular sectors. The compressive contacts are plotted in the angular range $[0,\pi]$ (upper part) and the tensile contacts in the range $[0,-\pi]$ (lower part). We see from Fig. 6 that the distribution is anisotropic similar to that found in a non cohesive granular medium. For the initial state, contacts are orientated with a quasi-homogeneous manner for weak adhesion value. Unlike for strong adhesion and for two types of effort, two particular directions of ±45° with respect to the compression axis appear on the diagram. This "bi-modal" distribution of contact directions has also been observed for non cohesive particles deposited in the gravitational field [4]. Here we observe that this effect is much more important for high adhesion values. So we have a highly structured contact network for values of z>4.

Solid fraction: To complete the examination of the coordination number, we show the solid fraction (density), i.e. the fraction of space occupied by the disks, as a function of adhesion index. The solid fraction is calculated from:

$$\rho_s = \frac{S_{particle}}{S_{REV}} \tag{4}$$

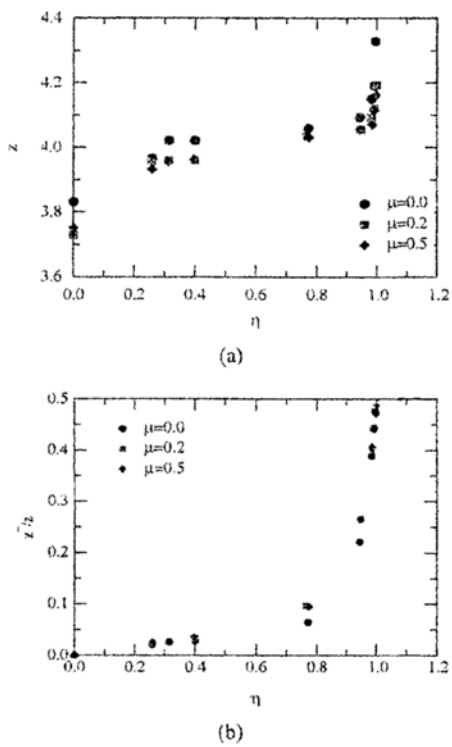

Fig. 5. (a) Evolution of coordination number z and (b) evolution of coordination number for the tensile contact z^- normalized by z as function of the adhesion index η for three different values of friction coefficients μ.

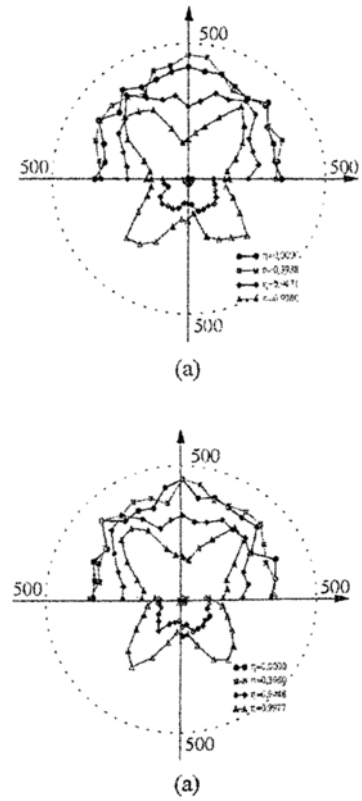

Fig. 6. Polar diagram of the distribution of contact directions for compressive $[0,\pi]$ (upper) and tensile $[0, -\pi]$ (lower) contacts for (a) non friction case and (b) μ = 0.5.

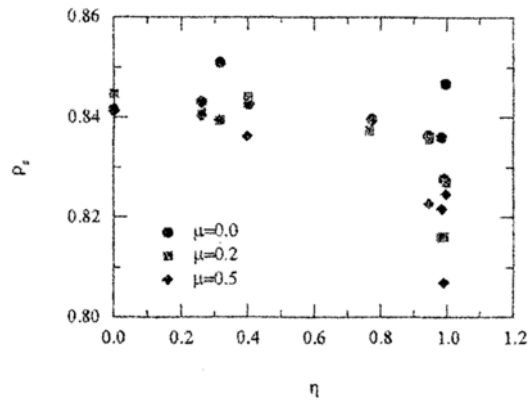

Fig. 7. Evolution of the compactness ρ_s as function of η for three values of friction coefficients.

where S_{REV} is a representative elementary area (or volume in 3D) and $S_{particle}$ is the area (volume for 3D) of particles inside the S_{REV}. In all simulations we chose an S_{REV} to contain approximately 350 particles. Fig. 7 shows the solid fraction ρ_s as a function of the adhesion index η and for three different values of friction coefficient μ. Observe the adhesion has a small influence on the compactness, except at high values of η (close to 1) for which the density decreases slightly. Otherwise, the higher the friction, the lower the compactness that occurs. Indeed, in the preparation phase, a small friction force favors the rearrangements of particles, and allows the system to reach a more compact state.

Force networks: The transmitted efforts through the contacts are represented by the lines which join the centers of disks in contact and for which the thickness is proportional to the value of the normal force. The black lines represent compressive efforts and the gray ones tensile efforts. The aspects of the force network are quite similar to those of non cohesive media (inhomogeneous, filamentary structure) [1]. The tensile effort doesn't develop uniquely for the medium and high values of the surface energies, η>0.8 although the system is under compression in all directions; see in Fig.8, for the strong cohesive system. In this figure, we see the appearance of the strong force chains both in compressive and tensile networks for which the magnitude of the largest tensile and compressive force are comparable and are strongly correlated. Indeed, for η>0.9, observe that the force chain for tensile forces develops in parallel to the compression and some particles are in equilibrium from tensile forces only (crystallization).

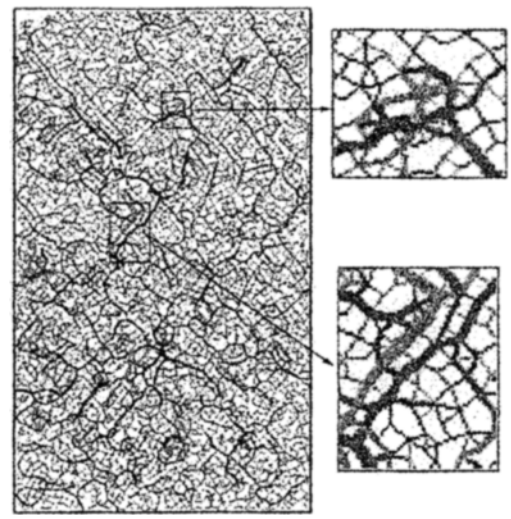

Fig. 8. Network of normal forces of contact in a strongly cohesive system with η = 0.9910 and μ = 0.5 at the equilibrium state.

Tensile pressure: We saw that the supplementary densification of the very strongly cohesive system is accompanied by a network of tensile contacts comparable to the compression contacts. The tensile contacts contribute negatively to the average pressure of the medium. The average pressure is given classically by

$$p = \frac{\sigma_I + \sigma_{II}}{2} \tag{5}$$

where σ_I and σ_{II} are the eigenvalues of the stress tensor which is defined as [14]:

$$\sigma_{ij} = \left\langle l_i^\alpha f_j^\alpha \right\rangle \tag{6}$$

Here l^α is the vector joining the particle centers and f^α the magnitude of contact force. The stress, or the average negative pressure p^-, is determined by this expression when restricted only to tensile contacts. The total pressure is given by the sum of these pressures, $p = p^+ + p^-$.

The evolution of the average negative pressure p^- can be normalized in relation to the average pressure p as a function of η (Fig. 9). We see that p^- remains quite low (η <0.8) except when η is very close to 1. For the large surface energies, p^- increases rapidly as a function of η due to self-stress configurations, although the system is subjected to compressive forces in all directions. Note also that each point in Fig. 9 is the result of a separate simulation according to the

procedure described above. We remark again that the negative pressure due to tensile force increases significantly only for the high adhesion values.

Distribution of normal forces: Both compressive and tensile forces are inhomogeneously distributed and show a large variability as for a non cohesive system. The maximum value of the contact force is more than 5-8 times the average value of normal force for all the systems studied with differing values of the surface energy. For small values of adhesion, the resultants of the normal force distribution are separated into two parts according to the average value of effort [16, 17]. For the strong values of adhesion, we can distinguish only one part which the distribution of the probability of the large normal forces (in absolute value) falls off exponentially with slightly different exponents for compressive and tensile forces (Fig. 10). This probability distribution of forces, both tensile and compressive, has the same form as in non cohesive media. We note that considering all the contacts in the sample, approximately 60% have a normal contact force lower than the average value, for every surface energy considered.

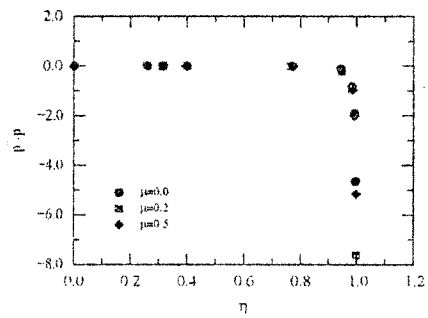

Fig. 9. Negative pressure p- due to the tensile force normalized by the average pressure p as a function of η for three different friction coefficients.

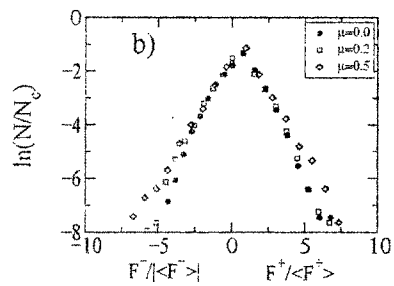

Fig. 10. Histogram in semi-logarithm of probability of normal forces normalized with respect to their normal average in each force type (compressive and tensile) for three different friction coefficients in strong cohesive system.

5. Conclusion

The numerical analysis presented on cohesive granular packing subject to compressive loading in all direction suggests the existence of three regimes that occur depending on the adhesion index η:

- The regime of *geometrical rearrangement* for $0<\eta<0.3$: In this regime, the adhesive character of the interparticle contacts mainly influences the coordination number z which increases with η for reaching the particular value of 4 for $\eta \leq 0.3$. There are almost no tensile forces in the medium (hence, no tensile pressure) and the distribution of normal direction of contact is similar to that in non cohesive media.
- The regime of *contacts reorganization* for $0.3<\eta<0.8$: The number of tensile contacts evolves with η but the coordination number remains nearly equal to 4. In this way, the compressive contacts are transformed into tensile contacts in this regime.
- The regime of *force reorganization* for $\eta>0.8$ (high values of η): Here the coordination number increases beyond four in two dimensions and the medium gets more textured as also the tensile forces due to the self-stress configuration are present in the system. Indeed, the negative pressure due to tensile contacts increases rapidly with η.

Nomenclature

Roman symbols

a : Contact surface
k : Contact stiffness
f_n : Normal force of contact
f_t : Tangent force of contact
F_c : Threshold tensile force
p : Pressure
$p(\theta)$: Statistical distribution of the normal direction of contact
r : Effective radius of the curvature of contact
S_{REV} : Representative elementary surface
v_t : Relative slide velocity
z : Coordination number

Greek symbols

α_n : Normal damping coefficient
β : Tangential Viscosity
δ : Overlap
γ : Surface or adhesive energy
η : Adhesion index

μ : Friction coefficient
ρ_s : Solid fraction
σ_{ij} : Stress tensor

References

[1] F. Radjai, D. Wolf, M. Jean and J. J. Moreau, Bimodal character of stress transmission in granular media, *Phys. Rev. Lett.* 80 (1998) 61.

[2] M. Oda, T. Sudoo, Fabric tensor showing anisotropy of granular soil and its application to soil plasticity, *Powders and Grains. 89* (1989) 155-161.

[3] B. Cambou, , From global to local variables in granular media, *Powders and Grains. 93* (1993) 73-86.

[4] F. Calvetti, G. Combe and J. Lancier, Experimental micromechanical analysis of a 2D granular material: relation between structure evolution and loading path, *Mechanics of Cohesive and Frictional Materials*. 2 (1997) 121-163.

[5] B. Cambou and M. Jean, Micromécanique des Matériaux Granulaires, HERMES Science Publications, (2001).

[6] J-R. Cho and H-W. Lee, A Petrov-Galerkin Natural Element Method Securing the Numerical Integration Accuracy, *J. of Mech. Sci. and Tech. (KSME Int. J.)* 20 (1) (2006) 94-109.

[7] M. P. Allen and D. J. Tildesley, *Computer Simulation of Liquid*, Oxford Science Publications, (1987).

[8] K. L. Johnson, K. Kendell and A. D. Roberts, Surface energy and the contact of elastic solids, Proc.Royal Soc. London A, 324 (1971) 301-313.

[9] S. Roux, Quasi-static contacts, *Physics of Dry Granular Media.* (1998) 267-184.

[10] J. Schäfer, S. Dippel and D. E. Wolf, Force schemes in simulations of granular materials, *J.Phys.I France*, 6 (1996) 5-20.

[11] F. Radjai, Multicontact dynamics, *Physics of Dry Granular Media.* (1998) 305-312.

[12] S. Luding, Collision & contacts between two particles, *Physics of Dry Granular Media.* (1998) 285-304.

[13] F. Radjai and D. Wolf, Features of static pressure in dense granular media, *Granular Matter.* 1 (1) (1998) 3-8.

[14] N. P. Kruyt and L. Rothenberg, Micromechanical definition of the strain tensor for granular materials, *Journal of Applied Mechanics.* 118 (1996) 706-711.

[15] H. Troadec, F. Radjai, S. Roux and J.-C. Charmet, A model for the statistics of local fabrics in granular media, *Powders and Grains.* (2001) 25-28.

[16] F. Radjai, M. Jean, J. J. Moreau and S. Roux, Force distributions in dense two dimensional granular systems, *Phys.Rev.Letts.* 77 (2) (1996) 274-277.

[17] F. Radjai, Dynamique des rotations et frottement collectif dans les systèmes granulaires, Ph.D. thesis, (1995).